SolarPACES 2022, 28th International Conference on Concentrating Solar Power and Chemical Energy Systems
Advanced Materials, Manufacturing, and Components
https://doi.org/10.52825/solarpaces.v1i.673

Published: 12 Feb. 2024

Seasonal Performance Characterization of a Gen3 Particle-Based Concentrating Solar Plant with a Spatially Resolved Transient Thermal Storage Model

Kaden Plewe[1][https://orcid.org/0000-0002-8682-6879], Dongmei Chen[1][https://orcid.org/0000-0002-3260-9385], Jeremy N. Sment[2][https://orcid.org/0000-0003-4700-7544], and Clifford K. Ho[2][https://orcid.org/0000-0002-2994-9450]

[1] The University of Texas at Austin Department of Mechanical Engineering, USA

[2] Sandia National Laboratories, USA

Abstract. Particle-based Gen3 Concentrating Solar Power (CSP) can be paired with high-temperature power cycles (>700 °C) and can have built-in long duration (≥10 hours) thermal energy storage if the working particles are stored properly in thermal energy storage bins. Although high-temperature and long-duration thermal energy storage can mitigate daily intermittencies in solar irradiation, seasonal variability in local meteorological conditions can still have a significant impact on the overall performance of CSP systems. Aside from daily cloud coverage affecting incident solar radiation, wind speed and ambient temperature are also significant variables regarding system heat attenuation, component efficiency, and overall solar conversion efficiency. In this work, we present simulation results for a Gen3 CSP prototype system in operation over four weeks throughout the year in Albuquerque, NM. The meteorological conditions are taken directly from the TMY3 data at the Albuquerque International Sunport, where the hourly Direct Normal Irradiation (DNI), wind speed, and ambient temperature are of particular interest. An investigation of the sensitivity of individual components like storage and ducting to the local meteorological conditions is provided and extended to the overall performance of the CSP system. The results from this study show that the particle inlet temperature at the particle-to-sCO_2 heat exchanger can change as fast as 30 °C/min under standard operation in a passive mode.

Keywords: Dynamic System Modelling, Particle Thermal Storage, Gen3 CSP

1. Introduction

The techno-economic modeling and forecasting of CSP and hybrid plants as a step toward justifying cost, design, and siting is a well-established procedure for Gen3 CSP technologies. Techno-economic analysis for Gen3 particle technology in particular has indicated a path toward achieving a levelized cost of electricity (LCOE) near 0.05$/kWh [1]. Some of the most influential parameters in the techno-economic feasibility of particle-based Gen3 CSP plants are the receiver efficiency, storage duration and capacity, and heat exchanger effectiveness. Hence, the way that these components behave under dynamic operating conditions, due to transient meteorological conditions and component-level heat attenuation, may significantly impact the operating performance and capacity factor of the plant.

Thermodynamically, maintaining accurate control of the sCO_2 turbine inlet temperature at the highest possible temperature is critical for maintaining high cycle efficiencies. But maintaining steady conditions at the heat exchanger and turbine inlet (i.e. ensuring CO_2 remains

supercritical) is particularly important for ensuring the integrity and performance of the supercritical turbomachinery equipment [2], [3]. This has been the motivation for the dynamic modeling and control of particle-to-sCO_2 heat exchangers and particle receiver technology. In [4], a dynamic model for a shell-and-plate particle-to-sCO_2 heat exchanger was used to apply feedback and feedforward control to regulate particle and sCO_2 outlet temperatures in response to instantaneous and linear changes in the particle inlet temperature. They were able to stabilize the outlet temperatures to within 19 °C of the setpoint temperatures in a three-minute window. Luu et. al. have also performed an extensive analysis on the flexible operation of sCO_2 power block operation in the presence of fluctuating supply in the solar block [5]–[7].In the body of work presented by Luu et. al., the system-level flexibility in response to a variable source is first studied and then followed up with dynamic modeling and controls development with the main objective of regulating the turbine inlet temperature.

The control of the particle receiver can provide early mitigation to fast variability in DNI if the temperature of particles leaving the receiver is regulated accurately. A demonstration of a temperature-controlled falling particle receiver (FPR) using a linear slide gate actuator was provided in [8] for an on-sun testing environment. It was found that temperature regulation with mass flow actuation in the falling particle receiver is highly challenging due to the dependence of thermophysical particle properties and thermal losses on ambient conditions and particle temperature. The particle receiver outlet temperature tolerance can be relaxed if electric heating is added prior to particles entering the heat exchanger since the hot thermal storage bin will inevitably add to and alter the transient temperature profile. Otherwise, a dynamic model for the particle receiver will need to be used in the control strategy to increase the robustness and accuracy of temperature regulation.

In this work, we model the primary heat exchange components from the particle receiver to the heat exchanger with a fluctuating solar input and ambient temperature. We simulate the system response to these fluctuations passively as a precursor to future work that will actively mitigate these fluctuations on the particle side using various control mechanisms. This is similar to what was done in [2] and [4], where dynamic models for the sCO_2 power block were simulated under variable conditions with a sub-hourly time step to evaluate component performance under the propagation of thermal fluctuations. However, we show here that the heat loss, especially in the hot thermal storage bin, adds complexity to the thermal fluctuation propagation and transient behavior at the heat exchanger; and this isn't well documented in existing literature.

Building upon findings provided in [9] and [10], we show here a more detailed analysis of the direct effect of meteorological fluctuations on component and system-level performance. In particular, the spatially resolved and transient thermal energy storage bin model is integrated into the G3P3 system model to better understand the importance of capturing the spatially resolved temperature profile in the storage bins in a predictive system model. This will contribute to the advancement of Gen3 CSP system operations in the following ways: 1) The hot thermal energy storage bin in the G3P3 system is modeled using a semi-analytical spatially resolved thermal model to capture the transient profile in the storage bin outlet temperatures and extend this feature to predictions for the system-level performance and 2) The system model is simulated with a time step of 10 seconds, which will enable the application of controls to mitigate fast transients and thermal ramp rates that are problematic for component operation and power dispatching.

2. Gen3 CSP System Model

The G3P3 system model was developed to capture the thermal energy transport of particles, and the individual component models are derived using appropriate simplifications and assumptions regarding their size, placement, and contribution to the overall thermal efficiency of the cycle. The system model outlined in Figure 1 is simulated in Simulink, and each individual

component is developed in MATLAB script using syntax that is compatible with Simulink compilers. It is also noted that the aim of this system model is to demonstrate the propagation of thermal fluctuations through integrated components, and not necessarily to reflect the expected system performance because system level controls are not investigated in depth in this work. However, the simulation of the G3P3 system with dynamic component models, particularly the receiver, hot particle storage bin model, and heat exchanger, provides valuable insight into the outlook of mitigatory operations and control algorithms that will be required to maintain a reliable power supply on an annual basis. This section will describe the modeling of major components in the G3P3 system.

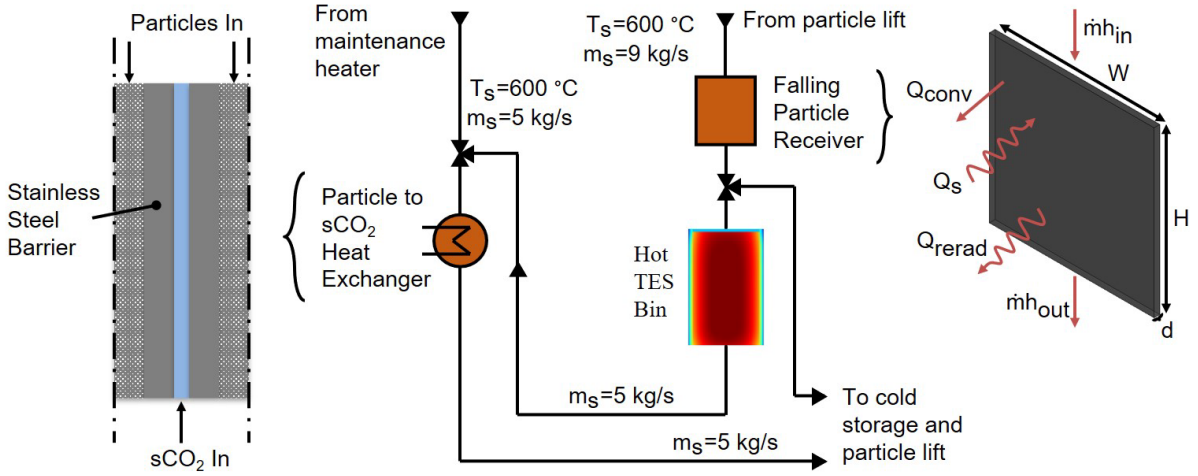

Figure 1. Section of Gen3 CSP system that is included in the model with assumed boundary conditions at the falling particle receiver inlet and heat exchanger inlet (at times when the hot TES bin is not discharging). Simplified models for the heat exchanger and falling particle reciever are shown on the left and right, respectively.

2.1. Falling Particle Receiver

The falling particle receiver is designed to receive upwards of 2 MWth from the heliostat field to maintain a 1 MWth throughput to the combined sCO_2 Brayton cycle. Here, the solar input fluctuates temporally depending on the hourly direct normal irradiation (DNI) that is obtained from TMY3 data over the prescribed time frame at the at the Albuquerque International Sunport. To mitigate these fluctuations, the mass flow rate of particles falling through the receiver can be controlled to maintain a constant outlet temperature as was done in [10], [11] and [8]. However, the fluctuation in solar energy acquired by the particles will ultimately need to be made up by some other source, such as electrical heaters or energy storage reserves. This paper is not focused on the controls problem that arises from these fluctuations, but rather the passive effect that meteorological fluctuations have on the operation of major components. Hence, we will model the falling particle receiver and sequential components as passive components with prescribed mass flow rates.

The solar input, Q_s, is computed using a simplified model for the heliostat field,

$$Q_s = nA_m\eta_m DNI \quad (1)$$

where n is the number of heliostats, A_m is the exposed area of each heliostat, η_m is the reflector efficiency, and DNI is the total direct normal irradiation obtained from the TMY3 dataset. The general representation of the particle control volume used to model solar radiation absorption is shown in Figure 1. The falling particle curtain is very thin (~4cm), so we approximate the control volume as a thermally lumped volume and account for the total absorbed solar irradiation, re-radiation, convective heat losses, and mass transport through the control volume. We

neglect the receiver enclosure and assume the re-radiation on both sides of the curtain to be equal, which is a conservative approximation because it neglects the heating of the enclosure material. Lastly, we assume that the curtain is opaque and a gray diffuse emitter, which is accompanied by an approximated solid volume fraction, ϕ_s, of 0.6. The governing energy equation for the control volume is then

$$V_r \rho_s c_{p,s} \phi_s \frac{dT_s}{dt} = \alpha_s Q_s - 2A_r \sigma \epsilon_s (T_s^4 - T_\infty^4) - 2A_r h_\infty (T_s - T_\infty) + \dot{m}_s c_{p,s} (T_s - T_{s,in}) \quad (2)$$

where T_s is the lumped particle temperature, T_∞ is the ambient temperature, $T_{s,in}$ is the temperature of particles entering the top of the receiver, and $\dot{m}_s$ is the particle mass flow rate. The other geometric and material properties, along with their values, are described in Table 1. Equation 2 can be solved using an appropriate numerical integration technique. Here, we used a midpoint method and a timestep of 10 seconds.

More advanced computational methods for modeling the falling particle receiver have been outlined in [11] and [12], and include discrete element Lagrangian and Eulerian-based models which capture the gas-solid interactions in the free-falling particles. These modeling efforts have led to the successful design optimization and testing of falling particle receivers that have efficiencies up to around 90% [11].

Table 1. Falling Particle Reciever Model Parameters.

	CARBOHSP® 40/70 Solid Particles	Source
specific heat, $c_{p,s}$	1250 J/kg-K	[13]
particle density, ρ_s	2000 kg/m^3	[13]
falling solid fraction, ϕ_s	0.6	[14]
particle curtain absorptivity, α_s	0.88	[15], [16]
Particle curtain emissivity, ε_s	0.92	[15], [16]
	Geometric Parameters	
aperture height, H	1.20 m	
aperture width, W	1.20 m	
falling particle curtain depth, d	0.042 m	
exposed falling curtain area, A_r	1.44 m^2	
falling curtain control volume, V_r	0.061 m^3	

2.2. Hot Particle Thermal Energy Storage Bin

The thermal heat loss through charge-hold-discharge cycles in the hot storage bin is modeled using a semi-analytical technique that consists of combining analytical conduction solutions for stagnant regions and numerical integration techniques for moving particle regions using a discretized Greens formula. A more in-depth description of the storage model can be found in [9] and [10]. This work presents the first integration of a spatially resolved transient storage model into a system-level configuration. Of particular importance here is the introduction of a time-dependent particle inlet temperature during the charging phase, which allows us to capture the passive effect of the solar input variability at the falling particle receiver. A transient inlet temperature (or transient inlet or outlet mass flow rate) will inevitable change the transient hot particle storage outlet temperature, which goes on to affect the operation of the particle-to-sCO2 heat exchanger. This is also left as a passive transfer of particles, although a particle heater or mixing will eventually be used to maintain a steady particle inlet temperature to the heat exchanger [10].

2.3. Particle-to-sCO$_2$ Heat Exchanger

We model the heat exchanger as a counterflow shell and plate heat exchanger, similar to the model considered in [4] and [17]. The spatial resolution and transient nature of the flowing

particles, sCO_2, and the separating stainless-steel barriers are captured, and in this paper, the inlet particle temperature comes directly from the hot storage bin without mixing or heating to represent the passive transient response of the heat exchanger. This is contrary to what was done in [10], where an electric heater heated the particles exiting the storage bin to maintain a constant inlet temperature and mass flow rate going into the heat exchanger, and the solar conversion efficiency varied by about 0.15 percent per °C change in particle outlet temperature. Other traditional heat exchanger control techniques can be applied to maintain operational setpoints for the particle and sCO_2 outlet temperatures, such as the feed-forward control strategy considered in [4].

A semi-discrete (continuous in time) method is used to simultaneously solve the system of linear equations representing the particle, T_s, supercritical CO_2, T_{CO2}, and stainless-steel barrier, T_m, temperatures. The governing energy equations are

$$\rho_s c_{p,s} \phi_s t_s \left(\frac{\partial T_s}{\partial t} + v_s \frac{\partial T_s}{\partial x} \right) = 2h_s (T_m - T_s) \tag{3}$$

$$\rho_{CO2} c_{p,CO2} t_{CO2} \left(\frac{\partial T_{CO2}}{\partial t} + v_{CO2} \frac{\partial T_{CO2}}{\partial x} \right) = 2h_{CO2} (T_m - T_{CO2}) \tag{4}$$

$$\rho_m c_m t_m \frac{\partial T_m}{\partial t} = h_s (T_s - T_m) - h_{CO2} (T_m - T_{CO2}) \tag{5}$$

which are all semi-lumped element approximations with neglected vertical and horizontal conduction effects. The heat transfer coefficients for the particle-to-wall and sCO_2-to-wall convective heat transfer are approximated from previous studies that estimate heat transfer coefficients with 2D thermal models and Gnielinski correlations [17]–[20]. Otherwise, using a bulk temperature for the packed particle bed could be an issue since the effective conductivity in packed beds tends to be small (0.3-0.8 W/m-K). The plate height, H, width, W, and the number of banks were selected based on the nominal design points and are provided in Table 2 along with other geometric and thermophysical parameters.

Table 2. Heat Exchanger Model Parameters

	CARBOHSP® 40/70 Solid Particles	Source
specific heat, $c_{p,s}$	1250 J/kgK	[17]
packed particle density, ρ_s	3300 kg/m^3	[17]
solid fraction, ϕ_s	0.6	[18]
particle heat transfer coefficient, h_s	400 W/m^{2}K	[18]–[21]
	sCO_2	
specific heat, $c_{p,CO2}$	1250 J/kgK	[22]
packed particle density, ρ_{CO2}	800 kg/m^3	[22]
CO_2 heat transfer coefficient, h_{CO2}	3000 W/m^{2}K	[18]–[21]
	Geometric Parameters	
number of banks, N	33	
plate height, H	1.5 m	
plate width, W	0.6 m	
particle channel thickness, t_s	0.006 m	[18]
CO_2 channel thickness, t_{CO2}	0.001 m	[18]
metal barrier thickness, t_m	0.001 m	[18]

3. Seasonal Simulations

Seasonal variation in meteorological conditions is modeled using four representative weeks starting on December 21, March 21, June 21, and September 23 for winter, spring, summer, and fall, respectively. Annually, the ambient temperature varies from about -9 to 40 °C. This

invariably impacts the parasitic losses in the system and will eventually lead to a larger marginal load for particle heating. A time step of 10 seconds was used to capture the passive response of component state variables to the fluctuations in DNI. TMY3 data is aggregated over one hour time steps, so we have a limited representation of the fluctuations that occur on 10 s intervals. In future work, data from an on-site meteorological station will be used to eliminate the error accrued in predictions that use interpolated TMY3 data. Using interpolated TMY3 data does, however, give some representation of the larger magnitude fluctuations and is reflected in the component-level responses presented in this section. Figure 3 shows some representative characteristics of these fluctuations for state variables in the receiver, storage bin, and heat exchanger. The ramp rate of the particle inlet temperature at the heat exchanger is perhaps the most important variable in terms of power dispatching and reliability and is provided for the four seasonal simulations in Figure 2.

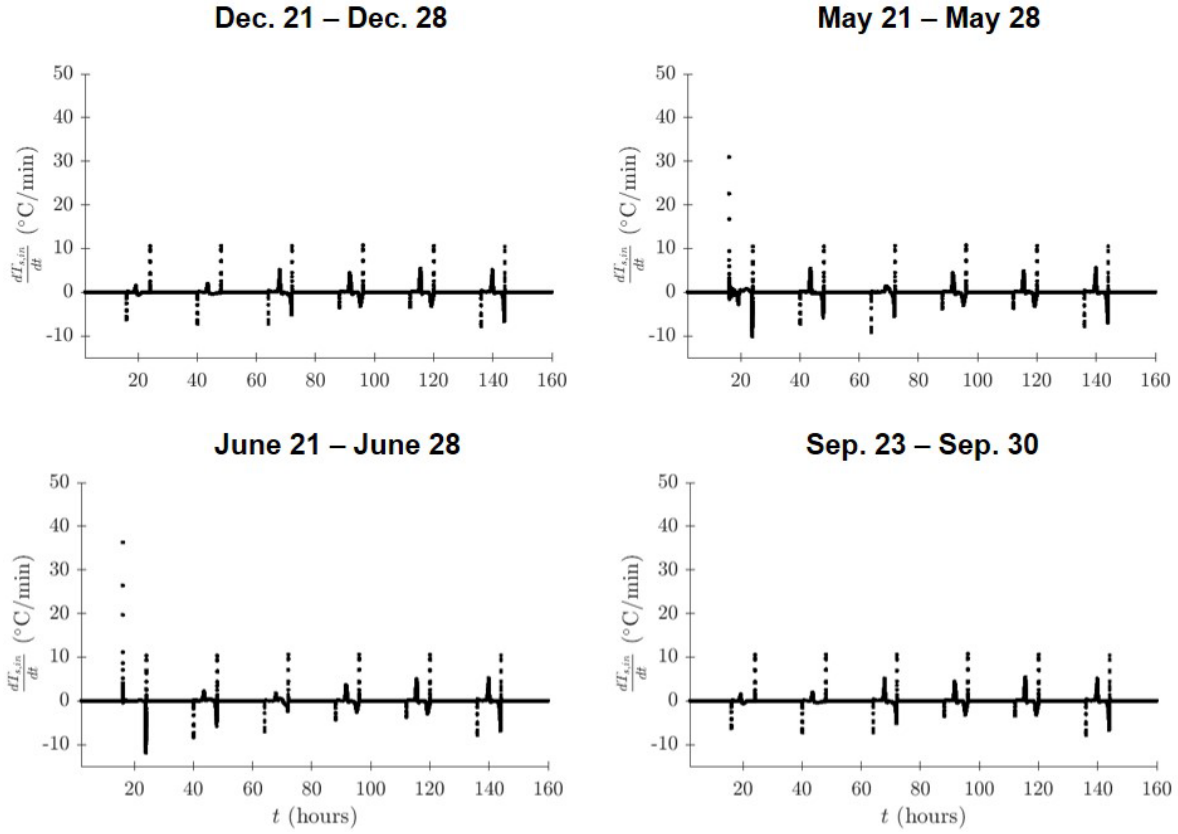

Figure 2. Thermal ramp rates for the particle inlet temperature at the particle-to-sCO_2 heat exchanger for week-long seasonal simulations in winter, spring, summer, and fall.

These simulations do not include active controls, and only show the passive response of components to fluctuations in the solar and particle temperature inputs. Three main components and free-fall ducts are modeled, and the cycle is completed with prescribed boundary conditions. This includes the inlet temperature and mass flow rate of particles entering the falling particle receiver (600 °C, 9 kg/s), the inlet temperature and mass flow rate of particles entering the heat exchanger when the hot TES bin is not discharging (600 °C, 5 kg/s), and the mass flow rates of particles entering and exiting the hot TES bin (9 kg/s and 5 kg/s, respectively).

In Figure 3, following the transition from left to right for each time horizon, it is evident that the fast transients occurring at the heat exchanger are introduced by the heat attenuation in the hot thermal storage bin. This is because the heat loss that occurs over the total of 16 hours of charging and holding in the storage bin smooths the fluctuations in the TES particle inlet temperature. During discharge, where particles flow out of the bin at 5 kg/s, the transient profile is mainly a product of the thermo-physical process of funnel flow in the storage bin.

However, the changes in the aggregate capacity of the plant that can be projected from the sCO_2 outlet temperature in Figure 3 occur on a diurnal time scale, which is manageable for hybrid plants and dispatch entities. On sub-hourly time scales, operational limitations of the heat exchanger and—if included in the system—electrical heaters are of concern with respect to the fast fluctuations shown in Figure 3 and ramp rates shown in Figure 2. During operation, mitigating components and controls must be able to regulate the sCO_2 outlet temperature to sustain the integrity of components in the power block [2], [3] which requires a response time of up to around 30 °C/min based on the results presented here.

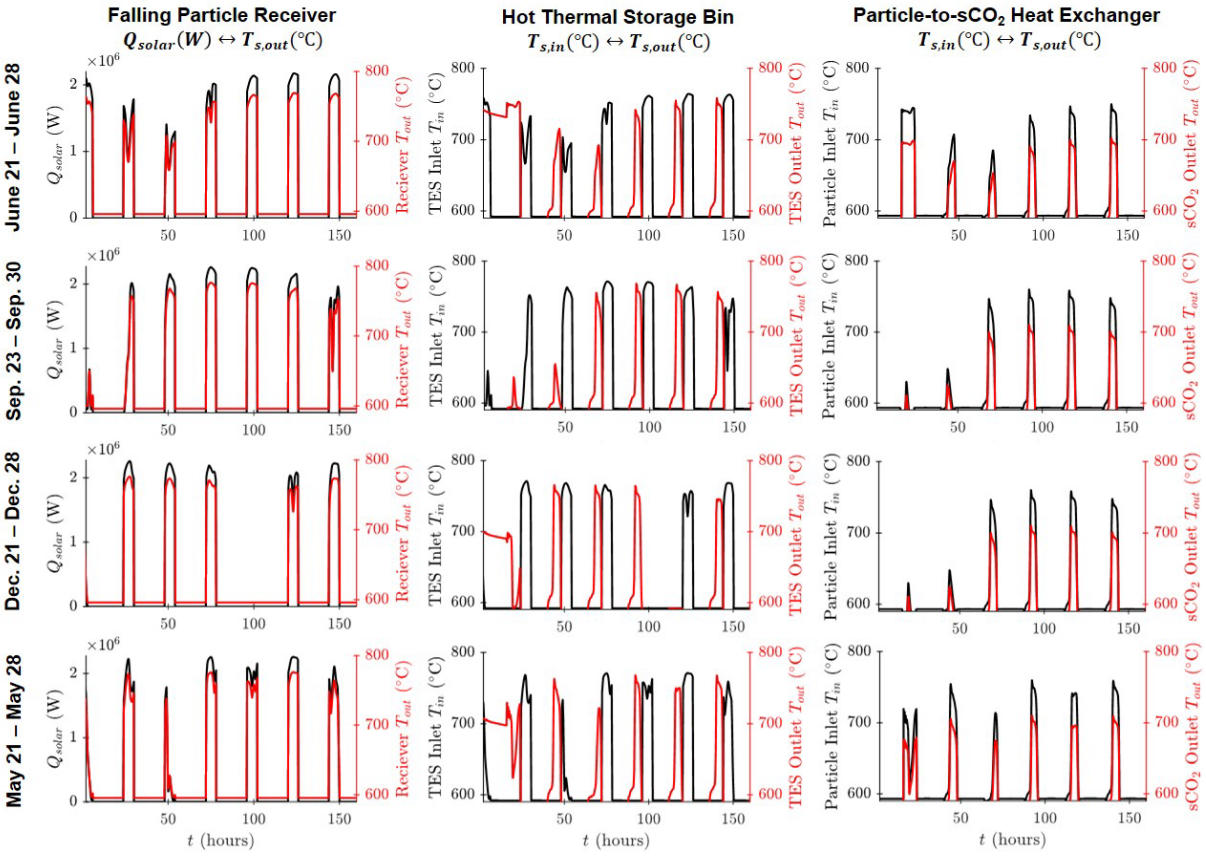

Figure 3. Simulation results for, from top to bottom, winter, spring, summer, and fall months in Albuquerque, NM. From left to right, inputs and state variables are shown for the falling particle receiver, hot particle thermal energy storage bin, heat exchanger.

4. Conclusions

In this work, a model was introduced that was developed to capture the transient behavior of critical components on the particle side of a Gen3 CSP plant. One of the main contributions is the inclusion of a high-temperature particle thermal storage model that captures the spatially resolved thermal attenuation during charge, hold, and discharge cycles, which is particularly important for flat-bottomed storage bins that discharge in a funnel flow pattern [9], [10]. In the results presented here, it is evident that the transient trajectory of the particles exiting the storage bin is highly sensitive to the particle inlet temperature. However, the transient characteristics that are introduced in the thermal storage bin will inevitably impact the rapid thermal ramp rates in the particle-to-sCO_2 heat exchanger if they are not mitigated. From the system model considered here, these ramp rates can be as fast as around 30 °C/min under standard operation scenarios in a passive state. Hence, the particle-to-sCO_2 heat exchanger will need to be controlled to regulate sCO_2 outlet temperatures under these conditions. In [4], the sCO_2 outlet temperature in scaled-down but similarly designed heat exchanger was regulated sufficiently

with a linear ramp rate of around 2 °C/min. Hence, further research, validation, and developments in modeling and controls will be necessary to ensure that the power block is insulated from rapid fluctuations on the particle side of particle-based Gen3 CSP plants. Ongoing efforts related to this work include the validation of the integrated thermal storage model under multi-cycle conditions and the implications of higher resolution and site-specific meteorological data. The framework that this model provides will then be used to develop controls based on the dynamic component models to mitigate the inherent thermal fluctuations identified herein.

Data availability statement

The data presented in this paper can be found online at git@github.com:kadenP/Plewe-SolarPACES2022.git

Underlying and related material

The underlying code base used in this work is currently held private under a restricted access contract.

Competing interests

The authors declare no competing interests.

Funding

This work is funded in part or whole by the U.S. Department of Energy Solar Energy Technologies Office under Award Number 34211 and 28711.

Sandia National Laboratories is a multimission laboratory managed and operated by National Technology and Engineering Solutions of Sandia, LLC, a wholly owned subsidiary of Honeywell International, Inc., for the U.S. Department of Energy's National Nuclear Security Administration under contract DE-NA0003525.

References

1. L. F. González-Portillo, K. Albrecht, and C. K. Ho, "Techno-economic optimization of CSP plants with free-falling particle receivers," Entropy, vol. 23, no. 1, pp. 1–24, 2021, doi: 10.3390/e23010076.
2. R. Singh, S. A. Miller, A. S. Rowlands, and P. A. Jacobs, "Dynamic characteristics of a direct-heated supercritical carbon-dioxide Brayton cycle in a solar thermal power plant," *Energy*, vol. 50, no. 1, pp. 194–204, 2013, doi: 10.1016/j.energy.2012.11.029.
3. S. J. Bae, Y. Ahn, J. Lee, S. G. Kim, S. Baik, and J. I. Lee, "Experimental and numerical investigation of supercritical CO2 test loop transient behavior near the critical point operation," *Appl Therm Eng*, vol. 99, pp. 572–582, 2016, doi: 10.1016/j.applthermaleng.2016.01.075.
4. M. Fernández-Torrijos, K. J. Albrecht, and C. K. Ho, "Dynamic modeling of a particle/supercritical CO2 heat exchanger for transient analysis and control," *Appl Energy*, vol. 226, no. March, pp. 595–606, 2018, doi: 10.1016/j.apenergy.2018.06.016.
5. M. T. Luu, D. Milani, R. McNaughton, and A. Abbas, "Dynamic modelling and start-up operation of a solar-assisted recompression supercritical CO2 Brayton power cycle," *Appl Energy*, vol. 199, pp. 247–263, 2017, doi: 10.1016/j.apenergy.2017.04.073.
6. M. T. Luu, D. Milani, R. McNaughton, and A. Abbas, "Advanced control strategies for dynamic operation of a solar-assisted recompression supercritical CO2 Brayton power

cycle," *Appl Therm Eng*, vol. 136, no. March, pp. 682–700, 2018, doi: 10.1016/j.applthermaleng.2018.03.021.
7. M. T. Luu, D. Milani, R. McNaughton, and A. Abbas, "Analysis for flexible operation of supercritical CO2 Brayton cycle integrated with solar thermal systems," *Energy*, vol. 124, pp. 752–771, 2017, doi: 10.1016/j.energy.2017.02.040.
8. N. Schroeder, H. Laubscher, B. Mills, and C. K. Ho, "Receiver outlet temperature control for falling particle receiver applications," *Proceedings of the ASME 2021 15th International Conference on Energy Sustainability, ES 2021*, pp. 1–7, 2021, doi: 10.1115/ES2021-62319.
9. K. Plewe, J. N. Sment, M. J. Martinez, C. K. Ho, and D. Chen, "Transient Thermal Performance of High-Temperature Particle Storage Bins." in SolarPACES 2020 Conference Proceedings, 2020.
10. K. Plewe, J. N. Sment, K. Albrecht, C. K. Ho, and D. Chen, "Transient System Analysis of a Gen3 Particle-Based CSP Plant with Spatially Resolved Thermal Storage Charging and Discharging." in SolarPACES 2021 Conference Proceedings, 2021.
11. B. H. Mills, C. K. Ho, N. R. Schroeder, R. Shaeffer, H. F. Laubscher, and K. J. Albrecht, "Design Evaluation of a Next-Generation High-Temperature Particle Receiver for Concentrating Solar Thermal Applications," *Energies (Basel)*, vol. 15, no. 5, 2022, doi: 10.3390/en15051657.
12. B. Mills, B. Schroeder, L. Yue, R. Shaeffer, and C. K. Ho, "Optimizing a falling particle receiver geometry using CFD simulations to maximize the thermal efficiency," *AIP Conf Proc*, vol. 2303, no. December, 2020, doi: 10.1063/5.0029331.
13. C. K. Ho, K. J. Albrecht, L. Yue, B. Mills, J. N. Sment, J. Christian, and M. Carlson, "Overview and Design Basis for the Gen 3 Particle Pilot Plant (G3P3)," in SolarPACES 2019 Conference Proceedings, 2019.
14. L. F. González-Portillo, R. Abbas, K. Albrecht, and C. Ho, "Analysis of optical properties in particle curtains," *Solar Energy*, vol. 213, no. October 2020, pp. 211–224, 2021, doi: 10.1016/j.solener.2020.11.012.
15. N. Siegel, M. Gross, C. Ho, T. Phan, and J. Yuan, "Physical properties of solid particle thermal energy storage media for concentrating solar power applications," *Energy Procedia*, vol. 49, pp. 1015–1023, 2014, doi: 10.1016/j.egypro.2014.03.109.
16. N. P. Siegel, M. D. Gross, and R. Coury, "The development of direct absorption and storage media for falling particle solar central receivers," *Journal of Solar Energy Engineering, Transactions of the ASME*, vol. 137, no. 4, pp. 1–7, 2015, doi: 10.1115/1.4030069.
17. K. J. Albrecht and C. K. Ho, "Design and operating considerations for a shell-and-plate, moving packed-bed, particle-to-sCO2 heat exchanger," *Solar Energy*, vol. 178, no. December 2018, pp. 331–340, 2019, doi: 10.1016/j.solener.2018.11.065.
18. K. J. Albrecht and C. K. Ho, "Design and operating considerations for a shell-and-plate, moving packed-bed, particle-to-sCO2 heat exchanger," *Solar Energy*, vol. 178, no. November 2018, pp. 331–340, 2019, doi: 10.1016/j.solener.2018.11.065.
19. G. Volker, "New equations for heat and mass transfer in turbulent pipe and channel flow," Int. Chem. Eng. Vol. 16, no. 2, pp. 359-368, 1976.
20. K. J. Albrecht and C. K. Ho, "Heat Transfer Models of Moving Packed-Bed Particle-to-sCO2 Heat Exchangers," *Journal of Solar Energy Engineering, Transactions of the ASME*, vol. 141, no. 3, pp. 1–8, 2019, doi: 10.1115/1.4041546.
21. M. Fernández-Torrijos, K. J. Albrecht, and C. K. Ho, "Dynamic modeling of a particle/supercritical CO2 heat exchanger for transient analysis and control," *Applied Energy*, vol. 226, no. May, pp. 595–606, 2018, doi: 10.1016/j.apenergy.2018.06.016.
22. P. Nikolai, B. Rabiyat, A. Aslan, and A. Ilmutdin, *Supercritical CO 2 : Properties and Technological Applications - A Review*, vol. 28, no. 3. 2019. doi: 10.1007/s11630-019-1118-4.